Available online at www.sciencedirect.com
SCIENCE DIRECT®
Acta Materialia 53 (2005) 297–302
Acta MATERIALIA
www.actamat-journals.com

Accurate determination of domain boundary orientation in $LaNbO_4$

O. Prytz [a,*], J. Tafto [b]

[a] Centre for Materials Science and Nanotechnology, University of Oslo, P.O. Box 1126 Blindern, N-0318 Oslo, Norway
[b] Department of Physics, University of Oslo, P.O. Box 1048, Blindern, N-0316 Oslo, Norway

Received 30 June 2004; received in revised form 15 September 2004; accepted 21 September 2004
Available online 26 October 2004

Abstract

The orientation relationship between ferroelastic domains in $LaNbO_4$ (with 0.5 at.% Sr) is studied by selected area electron diffraction and high-resolution electron microscopy. At room temperature the domains are related through a simple rotation of approximately 95° about the monoclinic [0 1 0] axis, and the interface between two adjacent domains is highly ordered. The domain boundary is found to be the (2 0 −5.10)/(5.10 0 2) planes of the two domains, in excellent agreement with our theoretical predictions. This orientation differs considerably from that predicted by more elaborate ferroelastic theory.

Keywords: High-resolution electron microscopy; Electron diffraction; X-ray diffraction; Ceramics; Interface structure

1. Introduction

Lanthanum orthoniobate ($LaNbO_4$) exhibits a diffusionless transformation of the second order upon cooling from a tetragonal to a monoclinic structure. This transformation has been reported to occur at approximately 500 °C [1]. At high temperatures the tetragonal space group is $I4_1/a$ [2] while at low temperatures it is monoclinic C2/c [3]. For easy comparison with the high temperature structure we may use a non-conventional I-centred monoclinic unit cell. The space group is then I2/c, and the structure may be viewed as a monoclinic distortion of the high temperature structure.

The changes in lattice parameters caused by this transformation result in an increase in lattice strain energy, giving rise to a domain structure similar to the twinning structures observed in many materials. These domains have indeed been referred to as *type III mechanical twins* [4], but are not crystallographic twins according to the conventional definitions. The orientations of two adjacent domains are not related through any operation of symmetry, but rather a simple rotation about the [0 1 0] axis which approaches 95.6° at room temperature [5].

The tetragonal to monoclinic transition of $LaNbO_4$ may be described as a ferroelastic 4/mF2/m transition using the notation of Aizu [6]. The observed domains are then ferroelastic domains corresponding to the two allowed orientation states resulting from this transition, and the spontaneous strain tensors of the two orientation states are related by the fourfold rotation symmetry [6].

Jian and Wayman [5] have analysed the tetragonal to monoclinic transition using the formalism of Aizu [6] and a method first presented by Sapriel [7], and predict that the boundary between two adjacent domains are the (2 0 −4.04)/(4.04 0 2) planes of the two domains [5]. They also present selected area electron diffraction (SAED) studies which they interpret as supporting this prediction. On the other hand, diffraction studies performed by Tsunekawa and Takei have indicated that the domain boundaries are the (2 0 −5.10)/(5.10 0 2) planes of the two domains [4].

* Corresponding author. Tel.: +47 22 84 06 84; fax: +47 22 84 06 51.
E-mail addresses: oystein.prytz@smn.uio.no (O. Prytz), jtaftoe@fys.uio.no (J. Tafto).

1359-6454/$30.00
doi:10.1016/j.actamat.2004.09.023

Jian and Wayman performed studies using high-resolution electron microscopy (HREM) that reveal a region of increased contrast between the two domains. Based on these observations, they concluded that that the boundary is diffuse with a transition region approximately 25 Å in width [5].

In the present work, we study the cell parameters of $LaNbO_4$ doped with Sr by X-ray diffraction, and the orientation of the domain boundaries using SAED. Furthermore, the region between adjacent domains is examined by HREM, and a simple method of calculating the orientation of the boundaries based on the lattice parameters is presented.

2. Experimental procedures

Polycrystalline samples were kindly provided by the Ioffe institute in St. Petersburg. The specimens were synthesized using cold crucible induction melting of a mixture of La_2O_3, Nb_2O_5 and $SrCO_3$ giving a nominal composition $La_{0.95}Sr_{0.05}NbO_4$.

Samples for transmission electron microscope (TEM) studies were prepared in two ways:

(a) Samples were ground in acetone in an agate mortar and deposited on a carbon film suspended on a copper mesh.
(b) Samples were mechanically polished before thinning in a Gatan Precision Ion Polishing System with twin argon-ion guns. A 4 kV gun voltage was used, and the beam was oriented at 8° relative to the sample surface.

HREM images were obtained from ground specimens, while the SAED studies were performed on both ion-milled and ground specimens. The SAED studies were performed in a JEOL 2000FX TEM, while the HREM studies were performed in a JEOL 2010F TEM with a field emission electron gun. Both instruments were operated at 200 kV acceleration voltage.

Energy Dispersive X-ray (EDX) analyses of the composition were performed in the JEOL 2000FX TEM with a Tracor Northern X-ray detector and SCANDNORAX EDX-analyser.

Samples for X-ray diffraction were prepared by crushing the material in ethanol and depositing the powder on platinum plates. A Siemens D-500 diffractometer with a scintillation counter and a hot stage was used to obtain diffraction patterns at 20 temperatures between 75 and 600 °C using Cu Kα ($K\alpha_1$ and $K\alpha_2$) radiation with a scanning step of 0.02°. In addition, measurements were performed at 20 °C in a Siemens D-5000 diffractometer with Cu $K\alpha_1$ radiation and steps of 0.0155°. The XRD data were refined using the General Structure Analysis System [8].

3. Experimental results

EDX analyses of the sample composition revealed a slightly lower Sr content than expected. The composition was found to be $La_{0.97}Sr_{0.03}NbO_4$ as opposed to the nominal composition $La_{0.95}Sr_{0.05}NbO_4$.

The samples exhibit extensive domain structures see Fig. 1. The domains vary in size; the smallest observed domains are less than 20 nm in width, while the largest observed domain size is more than 300 nm.

Fig. 2 shows a HREM micrograph of a boundary between two adjacent domains, obtained with the incident electron beam not exactly parallel to the [0 1 0] axis of the monoclinic lattice. A region of increased contrast is apparent between the two domains, as indicated in Fig. 2. A similar contrast region was observed by Jian and Wayman [5], and attributed to a gradual transition between the two domains. However, we observed that the width of this contrast region varies with the sample thickness (see Fig. 2) and tilt, and disappears when the incident electron beam is exactly parallel to the domain boundary. Fig. 3 shows a HREM micrograph of a domain boundary in the [0 1 0] projection and we observe no evidence of a transition region. We have thus demonstrated that the contrast is caused by an overlap of the domains with respect to the electron beam, an effect obviously depending on the sample thickness as observed in Fig. 2.

Even a small misorientation of the beam with regard to the boundary can cause a fairly large apparent transition region. Assuming a misorientation of 1°, a 15 Å ''transition region'' comparable to that observed in

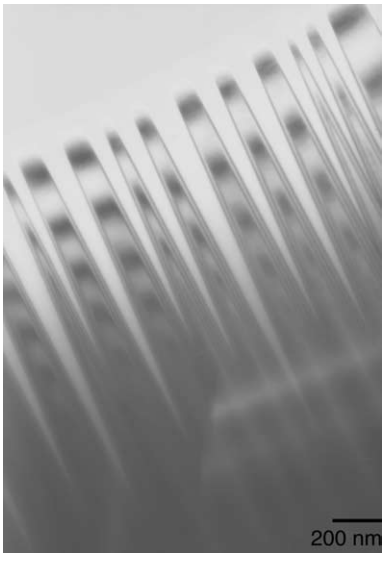

Fig. 1. Brightfield image of domains obtained somewhat out of the [0 1 0] projection, provided for the benefit of the aesthetically minded reader.

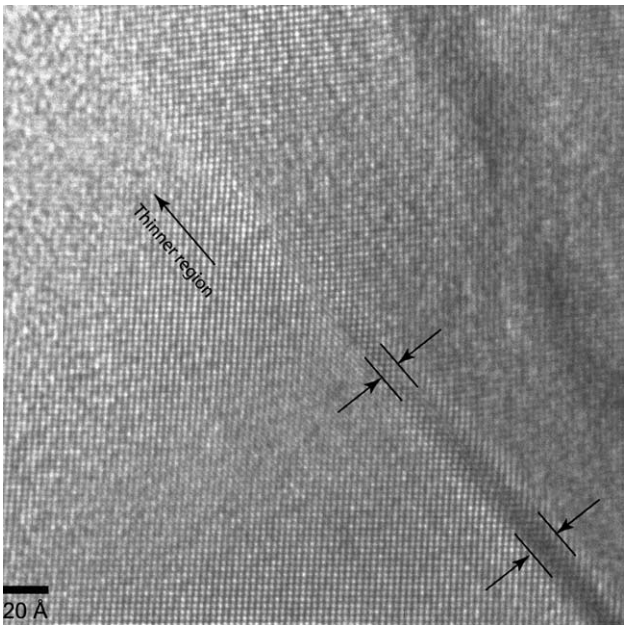

Fig. 2. HREM micrograph of a domain boundary. We note that the width decreases with decreasing sample thickness.

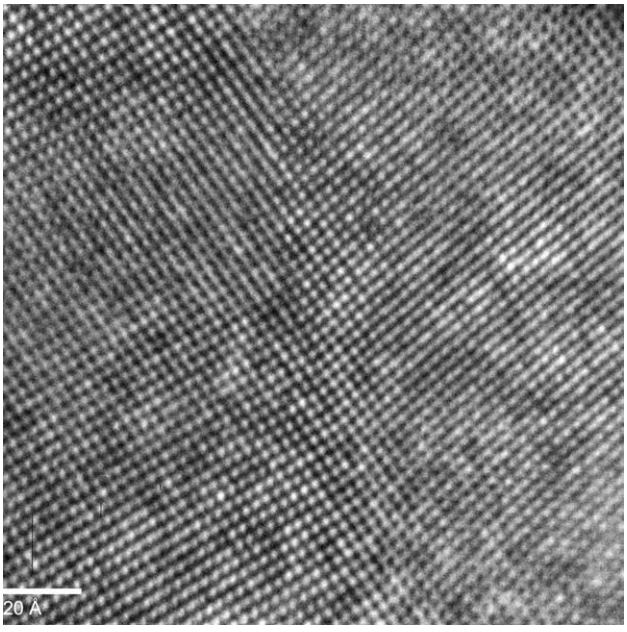

Fig. 3. HREM micrograph of a domain boundary. Notice that there is no indication of a transition region. The domain boundary is seen as an abrupt change in orientation of the lattice planes by viewing from the bottom left corner of the image.

Fig. 2 would correspond to a sample thickness of roughly 860 Å, which is quite plausible.

Fig. 4(a) shows an enlargement of part of the boundary in Fig. 3, while Fig. 4(b) shows a model of this domain boundary. These observations suggest a sharp transition from one domain to another, with the boundary in a first approximation being the (2 0 −6)/(6 0 2)

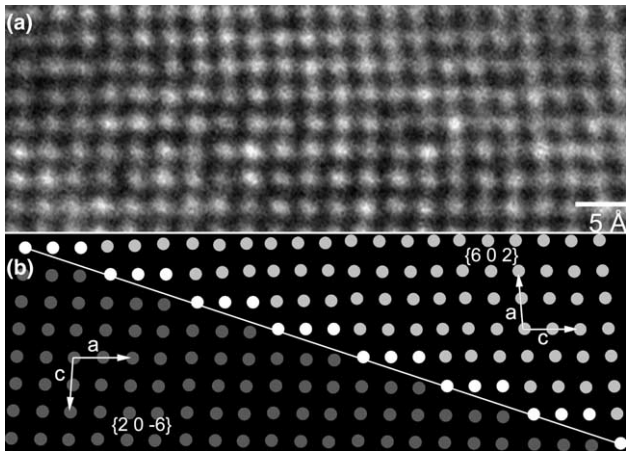

Fig. 4. (a) Close-up of the domain boundary. (b) Model of the boundary region in a. The boundary is oriented approximately parallel to the (2 0 −6)/(6 0 2) planes of the two domains.

planes of the two domains. It should be noted, however, that a local observation such as this can not be expected to fully reveal the true orientation of the boundary. In order to determine the true orientation, a more global approach is needed.

Tilting the sample into the [0 1 0] projection allows us to observe the domain boundary edge-on. An SAED pattern obtained from both sides of the boundary in this projection will exhibit a splitting of reflections consistent with the orientation relationship between the lattices of the two domains, see Fig. 5. The splitting indicates that the crystal structure of the two domains are related through a rotation of approximately 95° about the monoclinic [0 1 0] axis. The boundary between the domains must be two planes that are parallel in the two _domains, thus there should be no splitting of the corresponding reflections. We note that the diffraction pattern in Fig. 5(a) displays no such reflections.

Tilting the sample somewhat out of the [0 1 0] projection allows us to observe higher-index reflections. Fig. 6(a) shows a diffraction pattern obtained in this way, and we immediately note that there appears to be a splitting of all reflections, except the ones corresponding to the (4 0 −10)/(10 0 4) planes. However, closer examinations of these reflections reveal a slight splitting of this pair as well, see Fig. 6(b).

These observations suggest that the domain boundary is closely related to the (4 0 −10)/(10 0 4) planes, but with a slightly different orientation. To determine the exact orientation, we must find the coordinates of the intersect between the reciprocal lattices of the two domains. In order to do this, we consider the sketch in Fig. 6(c) which illustrates the diffraction pattern in the vicinity of the (4 0 −10)/(10 0 4) reflections.

We observe that the two triangles in Fig. 6(c) are geometrically similar; their sides are therefore related by some constant of proportionality. This constant is

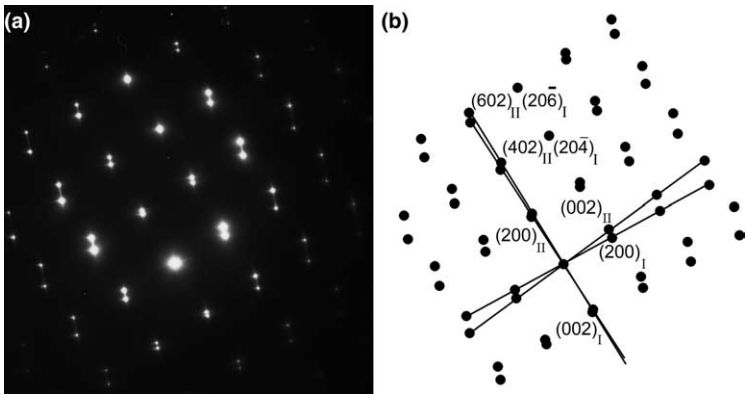

Fig. 5. (a) SAED pattern obtained at a domain boundary in the [0 1 0] projection. Note the splitting of the diffraction spots, indicating that the domains are related through a rotation of approximately 95° about the [0 1 0] axis. (b) Indexing of the diffraction pattern in a, the subscripts are used to separate the reflections from the two domains.

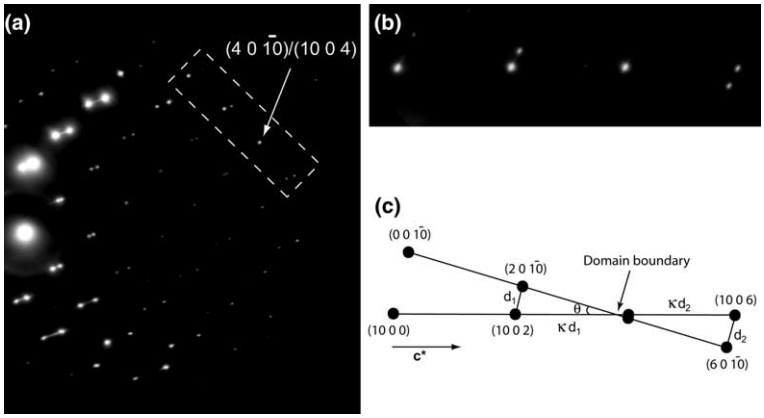

Fig. 6. (a) SAD diffraction pattern obtained from the Sr doped system with the sample tilted somewhat out of the [0 1 0] projection. Notice the apparent lack of splitting of the indicated (4 0 −10)/(10 0 4) reflections, suggesting that the domain boundary is closely related to these planes. The dashed box indicates the area enlarged in b. (b) Close-up of the area indicated in a. A slight splitting of the (4 0 −10)/(10 0 4) reflections is observed, indicating that the boundary is not quite parallel to these planes. (b) Sketch of the arrangement of diffractions spots in the vicinity of the (4 0 −10)/(10 0 4) reflections. The orientation of the domain boundary may be determined by identifying the coordinates of the intersect between the two lattices, indicated in the figure.

designated κ, and the distance between the (10 0 2) lattice site and the intersect is referred to as κd_1 while the distance between the intersect and the (10 0 6) lattice site is referred to as κd_2. Here d_1 and d_2 are the measured splitting of the two sets of diffraction spots adjacent to the (4 0 −10)/(10 0 4) reflections, as indicated in Fig. 6(c). The vector **c*** is a unit vector of one of the reciprocal lattices with length c^*.

The intersect is located at some point with index (10 0 ℓ), and studying Fig. 6(c) it is found that the value of ℓ may be determined by use of the following formula:

$$\ell = 2c^* + \frac{4c^*}{\kappa d_1 + \kappa d_2}\kappa d_1. \quad (1)$$

Exact measurements of d_1 and d_2 give a value of $\ell = 3.92c^*$, which leads to the conclusion that the observed domain boundary is the (2 0 −5.10)/(5.10 0 2) plane.

We performed X-ray diffraction at several different temperatures while heating the sample in order to study the evolution of the cell parameters as the system transforms from the monoclinic low temperature structure to the tetragonal high temperature structure. It is the reverse transition upon cooling from the high temperature phase which gives rise to the domain structure of the monoclinic phase.

X-ray diffraction was performed at 21 temperatures upon heating from 20 to 600 °C, giving detailed information on the changes in lattice parameters during the phase transistion. The refined values for the cell edges and the monoclinic angle β are given in Table 1 and illustrated in Fig. 7.

The room temperature cell parameters are in good agreement with the values obtained by Tsunekawa et al. [9] by neutron diffraction. Furthermore, we observe that the cell edges a and c converge towards

Table 1
Lattice parameters obtained at several temperatures from room temperature to 600 °C

Temperature/°C	a/Å(σ)	b/Å(σ)	c/Å(σ)	β(σ)	h(σ)
20	5.56868(9)	11.52963(17)	5.20451(8)	94.0834(10)	−5.007(1)
75	5.5578(4)	11.5277(8)	5.20264(29)	93.954(5)	−4.977(5)
150	5.5564(8)	11.5535(18)	5.2227(7)	93.713(10)	−4.982(10)
200	5.5497(7)	11.5729(17)	5.2315(7)	93.468(9)	−4.910(9)
300	5.5355(8)	11.6084(20)	5.2608(8)	92.962(11)	−4.879(13)
400	5.5113(9)	11.6466(22)	5.2996(8)	92.265(13)	−4.858(20)
450	5.4939(8)	11.6669(19)	5.3269(7)	91.788(11)	−4.865(21)
475	5.4771(9)	11.6786(23)	5.3408(9)	91.404(13)	−4.734(31)
480	5.4511(10)	11.6301(30)	5.3220(11)	91.318(16)	−4.691(39)
485	5.453(9)	11.631(20)	5.322(9)	91.321(19)	−4.652(47)
490	5.4710(9)	11.6816(27)	5.3517(10)	91.242(15)	−4.771(40)
495	5.4418(9)	11.6311(28)	5.3251(11)	91.175(15)	−4.645(41)
500	5.4368(8)	11.6376(24)	5.3283(9)	91.129(13)	−4.751(38)
505	5.4377(11)	11.6317(32)	5.3319(14)	91.078(18)	−4.684(54)
510	5.4344(7)	11.6317(20)	5.3326(8)	90.974(12)	−4.487(37)
515	5.4336(8)	11.6294(21)	5.3359(8)	90.951(12)	−4.540(39)
520	5.4297(8)	11.6367(22)	5.3367(9)	90.901(13)	−4.525(44)
530	5.4290(8)	11.6385(18)	5.3393(8)	90.816(11)	−4.341(38)
550	5.4126(8)	11.6490(18)	5.3495(8)	90.537(12)	−4.159(58)
575	5.4119(16)	11.6831(21)	5.4025(16)	90.04(6)	–
600	5.4093(10)	11.6891(14)	5.4033(10)	90.00(4)	–

The last column shows the predicted orientation parameter h, in (2 0 h)/(−h 0 2), for the domain boundaries based on Eq. (4). Predictions of h near the transition from monoclinic to tetragonal structure require cell parameters of utmost accuracy. Predictions for the two highest temperatures are therefore omitted.

approximately 5.40 Å in the high temperature case, while the b-axis approaches 11.69 Å and β is 90°. These results are in good agreement with those reported by David for the tetragonal phase of $LaNbO_4$ [2]. It is apparent from Fig. 7(a) and (b) that the largest changes in cell parameters occur around 500 °C, in reasonable agreement with the behaviour reported by Jian and Wayman [1]. We note, however, that the full tetragonal structure is achieved at approximately 600 °C, while previous reports indicate a tetragonal structure at 520 [1], 500 and 530 °C [2]. It is also observed that the cell parameters of this study exhibit a somewhat erratic behaviour in a region around 500 °C. However, we expect a hysteresis in the evolution of the cell parameters on cycling the temperature; this may explain the rather high transition temperature observed, and also the erratic behaviour of the cell parameters.

4. Discussion

Our HREM studies of the domain boundary reveal no indication of a disordered region between adjacent domains. On the contrary, the transition between domains seems to be highly abrupt.

In regard to the domain boundary orientation, the present study lends strong support to the early observations of Tsunekawa and Takei [4], as opposed to the calculations of Jian and Wayman [5] based on the work of Aizu [6] and Sapriel [7], and their interpretation of experimental data. On the whole, the formalism applied by Jian and Wayman is rather complex, and requires knowledge of the cell parameters of the material both before and after the transformation from the tetragonal to the monoclinic system. While this procedure is undoubtedly useful for more complicated systems and transitions, it seems excessive in the case of $LaNbO_4$. Add to this the discrepancy between the boundary orientations predicted by Jian and Wayman using this formalism, and the observations of the present study and the findings of Tsunekawa and Takei [4], it seems necessary to find other methods of predicting the orientation of the domain boundaries.

The domain boundary is a plane cutting through the sample in the monoclinic [0 1 0] direction, with an orientation designated (2 0 h)/(−h 0 2) in the two domains. In order to predict the value of h, we consider the sketch in Fig. 8 which shows the orientation of the crystal on both sides of a domain boundary in the monoclinic structure.

The length of the diagonal is d_1 and d_2 viewed from each of the two domains, and is given by the following set of equations:

$$d_1 = (kc)^2 + (2a)^2 - 2kc2a\cos\beta, \tag{2}$$

$$d_2 = (ka)^2 + (2c)^2 - 2ka2c\cos(180^\circ - \beta). \tag{3}$$

In order to maintain strain compatibility, the length of the diagonal must be equal viewed from either of the two domains. Setting Eqs. (2) and (3) equal and solving for k, allows us to obtain an expression for k which depends only on the cell parameters of the monoclinic phase:

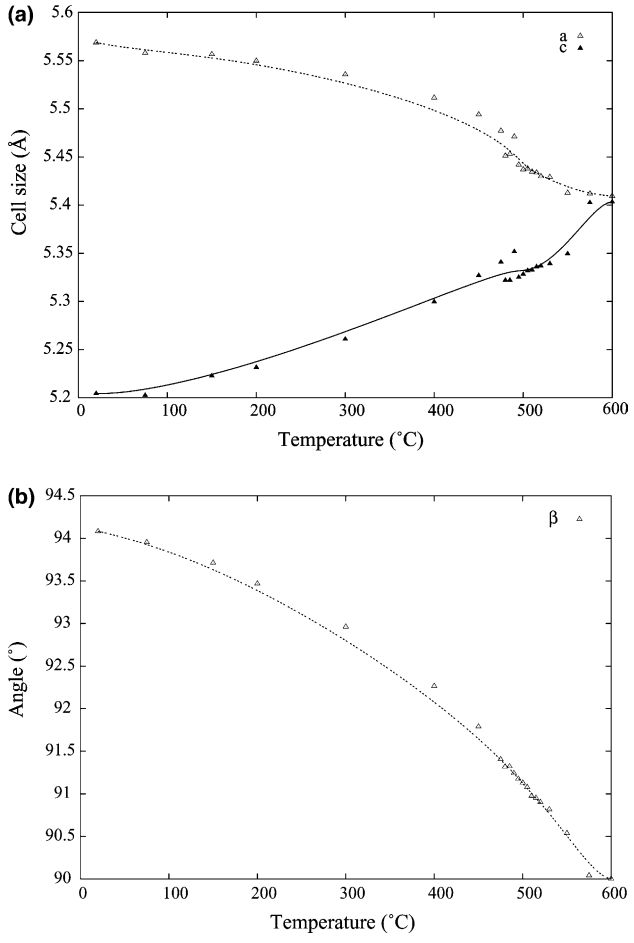

Fig. 7. The evolution of the cell parameters with temperature. The measurement errors are given in Table 1, and are too small to be reproduced in these figures. (a) The a and c axes. (b) The monoclinic angle β. The lines are provided to guide the eye.

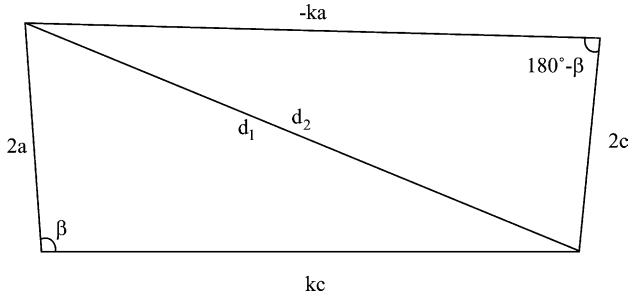

Fig. 8. The orientation of the domain boundary with respect to the crystal on either side of the boundary. Based on this sketch, the orientation of the boundary can be elucidated based on the monoclinic cell parameters.

$$k = \frac{-4ac\cos\beta \pm 2\sqrt{4a^2c^2\cos^2\beta - 2a^2c^2 + a^4 + c^4}}{a^2 - c^2}. \quad (4)$$

Using the cell parameters from the XRD studies performed, listed in Table 1, two values for k are obtained, corresponding to boundary orientations of (2 0 −5.01)/(5.01 0 2) and (2 0 0.799)/(−0.799 0 2) for the room temperature case. The first set of boundary orientations is in excellent agreement with our observations; the second set is merely symmetrically invariant to the first set.

Using this method and cell parameters from the XRD studies presented earlier, we may predict the evolution of the domain boundary orientation as the sample is heated. The predicted orientation parameter, h, is given in Table 1 for the different temperatures. We also note that Eq. (4) successfully predicts the convergence of the domain boundary to the (2 0 −2)/(2 0 2) planes at the transition from monoclinic to tetragonal structure. This corresponds to the annihilation of the domain structure.

5. Conclusion

The orientation relationship between ferroelastic domains in $LaNbO_4$ with 0.5 at.% Sr has been studied by selected area electron diffraction and high-resolution electron microscopy. At room temperature the domains are related through a simple rotation of approximately 95° about the monoclinic [0 1 0] axis, and the interface between two adjacent domains is highly ordered.

Furthermore, we have found the domain boundary orientation to be parallel to the (2 0 −5.10)/(5.10 0 2) planes of the two domains. We have also presented a simple model for predicting the boundary orientation which depends only on the monoclinic cell parameters. This model predicts an orientation at room temperature in excellent agreement with the experimental results of the present study and the previous study by Tsunekawa and Takei.

Acknowledgements

The authors are grateful to Drs. Y.M. Baikov and B.T. Melekh of the Ioffe Physico-Technical Institute, St. Petersburg, Russia, and Professor Truls Norby of the Department of Chemistry, the University of Oslo for providing the materials used in this study.

References

[1] Jian L, Wayman CM. J Am Ceram Soc 1997;80:803.
[2] David WIF. Mat Res Bull 1983;18:749.
[3] Tanaka M, Saito R, Watanabe D. Acta Crystallogr A 1980;36:350.
[4] Tsunekawa S, Takei H. Phys Stat Sol (a) 1978;50:695.
[5] Jian L, Wayman CM. J Am Ceram Soc 1996;79:1642.
[6] Aizu K. Phys Rev B 1970;2:754.
[7] Sapriel J. Phys Rev B 1975;12:5128.
[8] Larson AC, Von Dreele RB. General Structure Analysis System (GSAS), Los Alamos National Laboratory Report LAUR 2000;86–748.
[9] Tsunekawa S et al. Acta Crystallogr A 1993;49:595.